Ibn Al-Haitham Journal for Pure and Applied Sciences
Journal homepage: jih.uobaghdad.edu.iq
PISSN: 1609-4042, EISSN: 2521-3407
IHJPAS. 2026; 39(2)

Optimized Design and Numerical Modeling of 850 nm Vertical-Cavity Surface-Emitting Laser (VCSEL)

Rand Mahdi Khader[1*], and Shaimaa S. Mahdi[2]
[1,2]Department of Physics, College of Science for Women, University of Baghdad, Baghdad, Iraq
*Corresponding Author

Received: 22/June/2025
Accepted:4/December/2025
Published: 20/April/2026
doi.org/10.30526/39.2.4235

Abstract

0.850µm-wavelength 1D Vertical Cavity Surface Emitting Laser (VCSELs have matured as a short-distance optical communication light source that has small threshold currents, high modulation band width, and multimode fibers. In this paper, the design, simulation and analysis of an 850 nm oxide-confined 1DVCSEL have been presented using the Laser MOD tool from R-Soft software. The structure is a cylindrical-shaped design consisting of top and bottom DBRs, a multi-quantum well (MQW) active region, and an oxide aperture for transverse current for optical confinement. The numerical investigation gives rise to the spatial mode profiles, modal gain, threshold current, output power and far-field angle in terms of cavity or oxide aperture length, as well as amount of doping. For optimized performance, the cavity length was optimized to be 8.6 µm and the oxide aperture diameter 10 µm, resulting in single fundamental mode operation with high side-mode suppression. The far-field pattern is nearly Gaussian in shape and well suited for efficient coupling into multi-mode fibers. This work highlights the potential of Laser MOD for predictive design and optimization of VCSEL devices designed for high-speed data communication.

Keywords: Communication wavelength, DBR (Distributed Bragg Reflector), GaAs, In GaAs, Optical simulation, Quantum well.

1. Introduction

Although more than 40 years have passed since the emergence of vertical cavity surface-emitting lasers (VCSELs), which are one of the preferred semiconductor light sources for sensors and data transmission, as they have become a competitive source with high speed in optical communications, they are still under continuous development[1-3]. These lasers are characterized by distinct and unique properties in terms of power consumption and the ability to select their efficiency before manufacturing[4-5], in addition to low manufacturing costs, their single-mode output[6-7], and many features that make them ideal light sources for many applications and devices, including smartphones, cameras, self-driving cars, and others[8-12]. In order to utilize these advantages to the greatest possible extent in current and future applications, new designs and materials are being explored for VCSELs. This requires facing many challenges related to the design of modern VCSELs with improved performance. For this reason, design tools using computer-aided design (CAD) will enter as an essential support, as they play a major role in developing designs for prototypes, which eliminates the need for operations. Experimental manufacturing is expensive[13-15]. Due to the very high costs of manufacturing prototypes and the lack of practical experience, numerical simulation and modeling are very important in developing high-performance device designs. Through them, improved structures with desirable properties can be obtained in the short and long term. They can also give a comprehensive idea about the physical processes of the device, such as wavelength and others. This is done by

solving Maxwell's equations to obtain very accurate results for the electromagnetic field. Many different simulation methods have been used, such as the finite element method (FEM)[16], the finite integration technique (FIT), the finite difference time domain method (FDTD)[17,18], the transfer matrix method (TMM)[19] and many other methods. The main advantages of these methods are their ability to provide numerical modeling results with very high accuracy at a low cost[20]. One of the important challenges in developing VCSELs is obtaining the basic pattern with high power and high speed. Also, reaching the ideal design is expensive and requires a long time and effort. Therefore, a commercial program has been used to simulate the VCSEL and improve its performance[18-21]. Accordingly, a lot of effort has been put into improving the VCSEL design in recent years through simulations and experimental verification, for example. In 2020, a prototype VCSEL was developed by a group of researchers at the 850nm wavelength operating in a single mode, showing a highly efficient reduction in chromatic dispersion and an improvement in bandwidth, which enabled increased data transmission speeds over multimode fibers[22].In 2022, researchers presented a new model for a VCSEL operating at a wavelength of 850 nm using an anti-steering cavity structure, which facilitated data transmission speeds of up to 224 Gb/s while reducing chromatic dispersion and improving the frequency bandwidth in order to meet the increasing demands for optical communications at high speeds passing through multi-mode fibers[23]. Previous studies indicate that the majority of analytical model designs for VCSEL lasers relied on two- or three-dimensional simulations to describe the optical and thermal distribution within the device structure. However, these models require significant computational capabilities and take a long time, making them of limited use in the initial stages of device design. This research aims to present a one-dimensional (1D) model capable of providing accurate and rapid preliminary indicators of device performance before manufacturing. The one-dimensional (1D) approach was chosen in this research because it offers a balance between computational accuracy and modeling speed, making it a suitable tool for evaluating the impact of structural parameters, such as cavity length and oxide aperture diameter. Although the (1D) model does not provide all three-dimensional side effects, it is an important input for understanding the overall physical behavior of the laser and guiding subsequent advanced modeling. This research contributes to presenting a (1D) model simulation of a VCSEL laser at a wavelength of 0.850 μm, along with an analysis of the relationship between structural parameters and the optical performance of the device.

2. Materials and Methods

2.1. Theory

In the one-dimensional Vertical Cavity Surface Emitting Laser (1D VCSEL)[24] is simulated using the transfer matrix method (TMM) that is primarily based on the uniform grid Which refers to the spatial division of the geometric structure within the laser component in a regular manner into equal or almost equal grid cells or points.to assist in the equation solving on light distribution inside the laser[19,25]. This technique is applicable for numerical analysis of multilayer mirrors. Such It is based on constructive interference of light waves in two alternate layers of different refractive indices and whose thickness is almost equal to a quarter wavelength. This configuration is such a high reflection at a specified wavelength and the DBR an optimal mirror to be incorporated in the laser cavities for VCSEL[26,27]. The DBR working principle is based on the accumulation of partial reflections that correspond to the interfaces of the layers, in order to achieve optical interference, which results in an enhanced reflection[28,29].an approach considers reflectance for the thickness of each layer being a quarter of the wavelength This is so because the quarter-wavelength layers guarantee constructive interference with the light waves reflected from the interfaces of the several layers so that these waves reach the observation point in the same phase, so improving the total reflection coefficient and raising the efficiency of the laser cavity[19,30]. The light propagation in the laser structure is computed by solving Maxwell's equations. A set of solutions is developed which reduce the computational load for the full

resolution of specific cavity configurations. A subset of formulae, the photon rate equations, was employed to study favorable performance regimes in particular types of cavities. The interconnected optical, electrical, and thermal relationships in lasers are described by the following system of coupled rate equations, which links the dynamics of charge carriers (electrons and holes) and the dynamics of photons in the optical cavity. We begin with the carrier rate equation, which describes the charge carrier density in the active region with respect to time [19,31].

$$\frac{\partial N}{\partial t} = \frac{\eta_i I}{qV} - R_{nr}(N) - R_{sp}(N) - v_g g(N) S \quad (1)$$

Where $\frac{\partial N}{\partial t}$ represent the rate of carrier density change, N is the carrier density, η_i is the internal injection efficiency, I is the injection current, q is the electron charge, Vis the active region volume, R_{nr} is the non-radiative recombination rate, R_{sp} is the spontaneous recombination rate, v_g is the group velocity, g is the material gain coefficient, S is the photon density which is given by the following equation[19,31].

$$\frac{\partial S_{m,\omega}}{\partial t} = \left[G_{m,\omega} - \frac{1}{\tau_{m,\omega}}\right] S_{m,\omega} + R_{m,\omega}^{spon} \quad (2)$$

Where $S_{m\,\omega}$ represents the photon density for mode m at frequency ω, t is the parity time over which the photon density is calculated, G is the typical gain,τ is the half-life of the photons, and R is the spontaneous emission rate, which is given by the following equation[19]:

$$R_{m,\omega}^{spon} = \int dV |E_m|^2 \; u_{(\omega)} \quad (3)$$

The typical gain equation[10] is given by

$$G_{m,\omega=} \int dV \; |E_m|^2 \; \frac{C}{n_{eff}} \; g(\omega) \quad (4)$$

Where g is the material gain, dv is the differential volume element, E electric field, u is the spontaneous emission spectrum, C is the speed of light in a vacuum, and n_{eff} is the effective index. Losses caused by light propagation through the cavity sides can be calculated as given by[19].

$$\frac{1}{\tau_{m,w}} = \frac{1}{\tau_{mirror}} + \frac{1}{\tau_{scatter}} + \frac{C}{n_{eff,m}} \alpha_b \quad (5)$$

Where τ_{mirror} is the time constant associated with reflection loss in mirror,$\tau_{scatter}$is the time constant associated with the dispersion process, α_b is the modal absorption coefficient, the self-heating effect is described by solving the heat flow equation[19],

$$\left[C_L + \frac{3}{2} K_B (ne + nh)\right] \frac{\partial T}{\partial t} = \nabla\left(K_L \nabla T - \vec{S}_e - \vec{S}_h\right) + H \quad (6)$$

where C_L is the lattice heat capacity,$K_B$is the Boltzmann constant is the electron density, nh is the hole density, T is the absolute temperature, t is the time, K_L is the thermal conductivity coefficient, S_e is the electronic heat source, S_h is the hole heat source, H is the heat transfer coefficient[19]. Equations 1 to 6 represent an approach that can help develop and improve the VCSEL model by relying on electrical and optical phenomena.

2.2. VCSEL Model

Figure 1 shows the schematic design of an $Al_{(0)}\,Ga_{(1)}\,As$-based VCSEL operating at 850nm. In this structure, the multi-quantum-well (MQW) active region consists of three quantum wells. Two different materials were applied separately for the same design: one made of $In_{(0.01)}\,Ga_{(0.99)}\,As$ (Eg=1.409ev) and the other made of GaAs (Eg=1.424ev) with a thickness of 8nm and 8nm thick $Al_{(0.2)}\,Ga_{(0.8)}\,As$ barriers. DBRs consisting of $Al_{0.55}Ga_{0.45}\,As$ layers were used, the refractive index within each layer was controlled by the gradient of the chemical composition of the alloys, allowing the desired reflectivity to be achieved despite the use of the same material. 32 pairs of p-type upper DBRs and 36 pairs of n-type lower DBRs were used to form a highly reflective optical cavity to ensure high laser efficiency. An insulating layer was also used on both sides (oxide) to confine the current and optical field within the active region, which increases the efficiency of the device and improves its thermal stability.

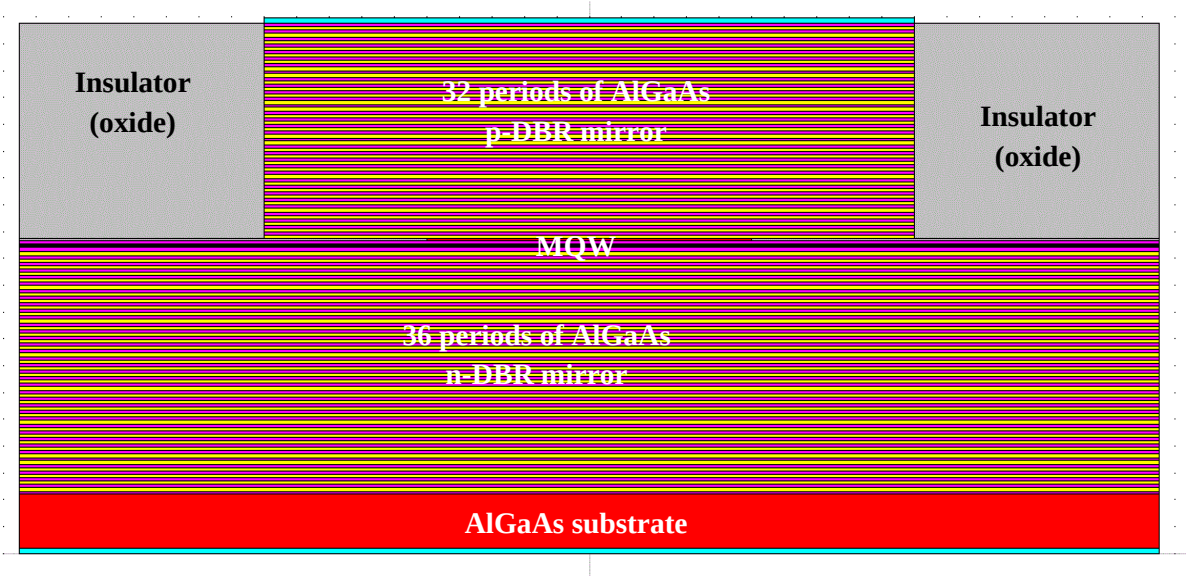

Figure 1. Schematic structure of the VCSEL device

3. Results

In this study, a VCSEL device was simulated with InGaAs and GaAs as the quantum well material and the optical behavior was explored at the wavelength of 850 nm. The findings showed similar optical properties of the two materials in which the optical power increased with the driving current and a clear peak of emission was observed in optical spectrum at about 850 nm, which proved the amplified optical response at the desired wavelength. The InGaAs based structure was found to respond to the optical response slightly better than the GaAs device, especially at higher temperature conditions, with GaAs having a slightly lower threshold current at room temperature.

The **Figure 2 a, b** indicates the distribution of the refractive index of a VCSEL structure built with GaAs and InGaAs quantum wells. The periodic change of refractive index depicts the high-low layers of refractive indices of distributed Bragg reflectors (DBRs). **Figure 3 a, b** shows the spatial distribution of the basic optical mode (Mode 0,0) at (Bias0). The two materials have a high concentration of optical power at y = 6 μm. The plots in **Figures 4 a, b** and **5 a, b** indicate the dependence of current (mA), voltage (V) and optical power (mW) versus temperature (300K and 350K) of both GaAs and InGaAs VCSELs and indicate LIV curves of the two cases. At 300 K, the GaAs device has a threshold current of 0.7 mA and a threshold voltage of 1.3 V and a peak power of 4.05 mW at 6.54 mA and 3.7 V, and the InGaAs equipment has a threshold current of 0.8 mA and the same threshold voltage and a peak power of 3.91 mW at 6.56 mA and 3.7 V. At 350 K, the GaAs device has a threshold current of 1.55 mA, threshold voltage of 1.3 V and a maximum power of 2.56 mW at 10 mA and 3.59 V and the InGaAs device had a threshold current of 1.5 mA, threshold voltage of 1.3 V and a maximum power of 3.19 mW at 10.2 mA and 3.59 V respectively. Such data indicate the power dependence on current and temperature of the individual materials. The **Figure 6 a, b** shows the dependence between present (mA) and temperature (K) of VCSEL. It demonstrates that the higher is the current, the higher the temperature of the device which influences its optical properties.

The transmission spectrum at bias (Bias0) in **Figure 7 a, b** displays oscillations at the beginning then it becomes stable and thereafter the abrupt peak at 0.850 um which is the design wavelength used in the emission appears. After the peak, the spectrum goes back to a transient stability and thereafter, strong oscillations are again experienced towards the end of the spectral range. **Figure 8 a, b** indicates the optical spectrum with 4 (3.7 eV) bias, in which there is a strong emission in the constructs at a wavelength of 0.850 μm indicating that the laser was successfully working at the wavelength of optical communications. It is also sharp and narrow at the peak, which proves

to be an efficient mono mode emitter. The gain spectrum of the simulated material when presented in **Figure 9 a, b** indicates that there is a sharp rise in gain at 0.850 µm. GaAs has a lower gain value compared to that of InGaAs, and its gain value is about 800 cm^{-1} and the GaAs gain value is about 600 cm^{-1}. **Figure 10 a, b** illustrates mode gain of the basic mode at Bias 4(3.7 V) where a definite gain improvement is realized at a wavelength of approximately 0.87µm that means the basic mode is effective at the wavelength.

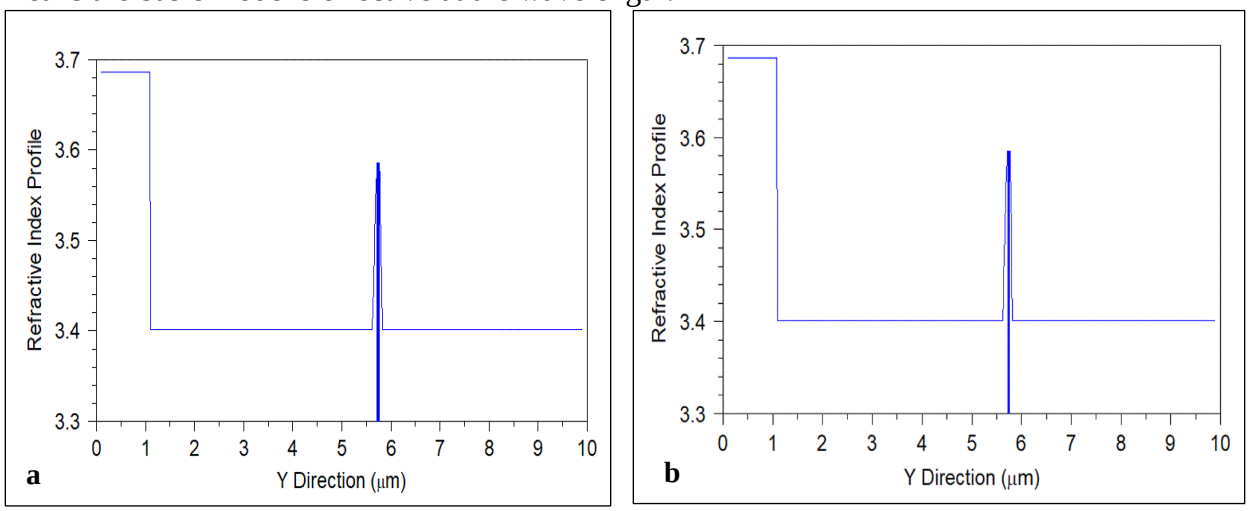

Figure 2. Refractive Index Profile a. (GaAs) , b. (InGaAs).

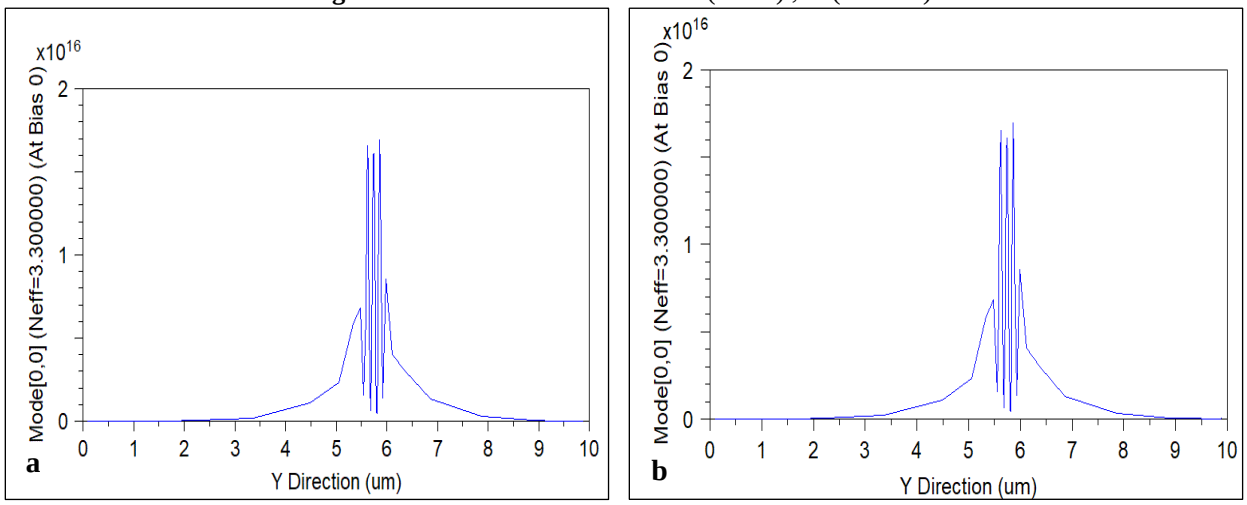

Figure 3. Mode (0,0) (Neff=3.300000) (At Bias 0) a. (GaAs) ,b. (InGaAs).

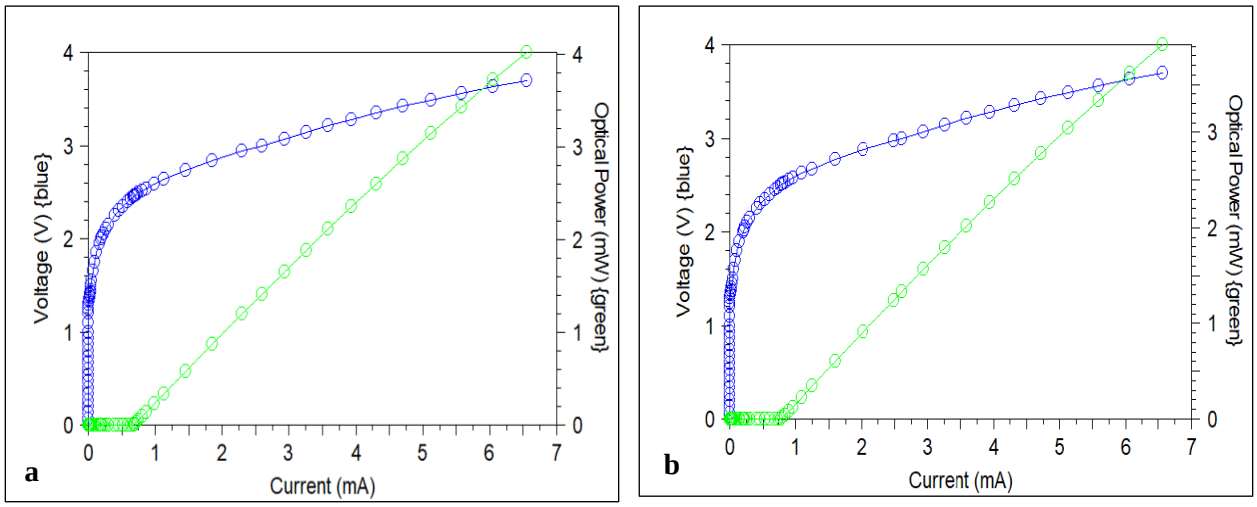

Figure 4. Light & Voltage vs Current (at T=300k) a. (GaAs) , b. (InGaAs).

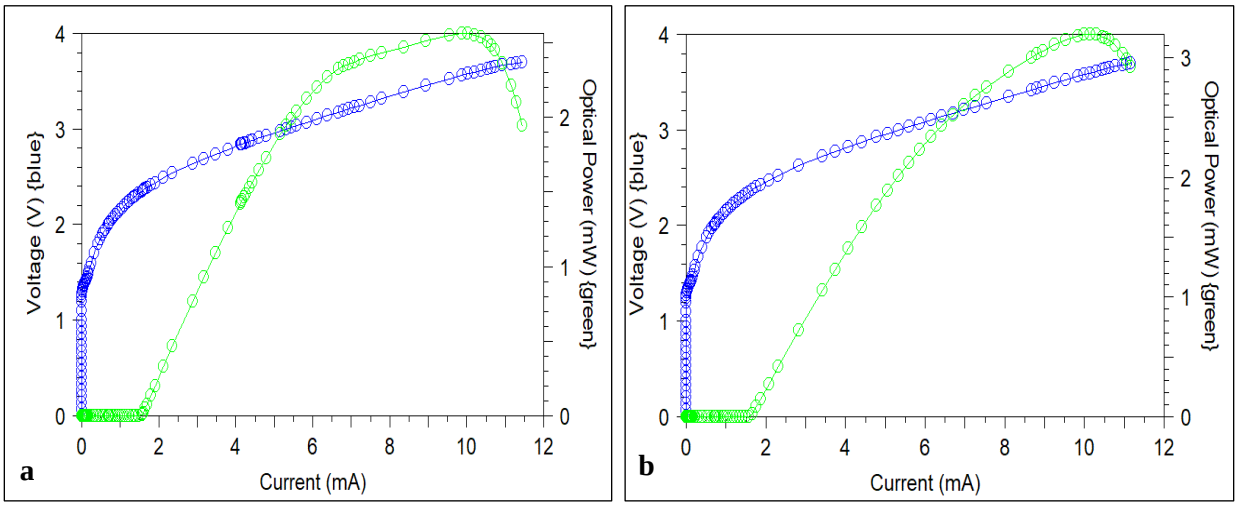

Figure.5. Light & Voltage vs Current (at T=350k) a. (GaAs), b. (InGaAs).

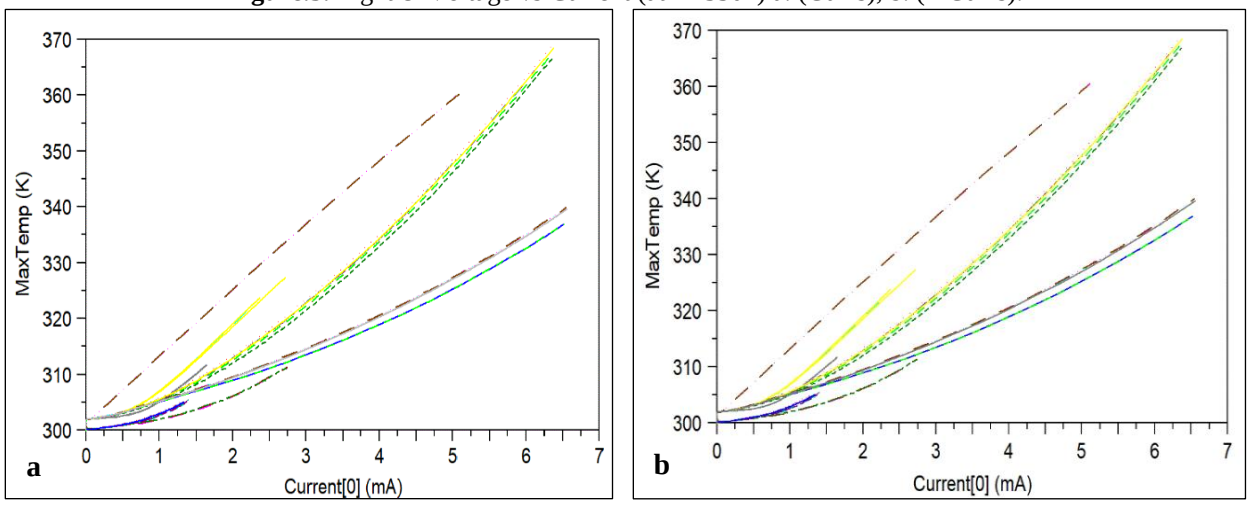

Figure 6. Max Temperature vs Current (0) a. (GaAs) , b. (InGaAs).

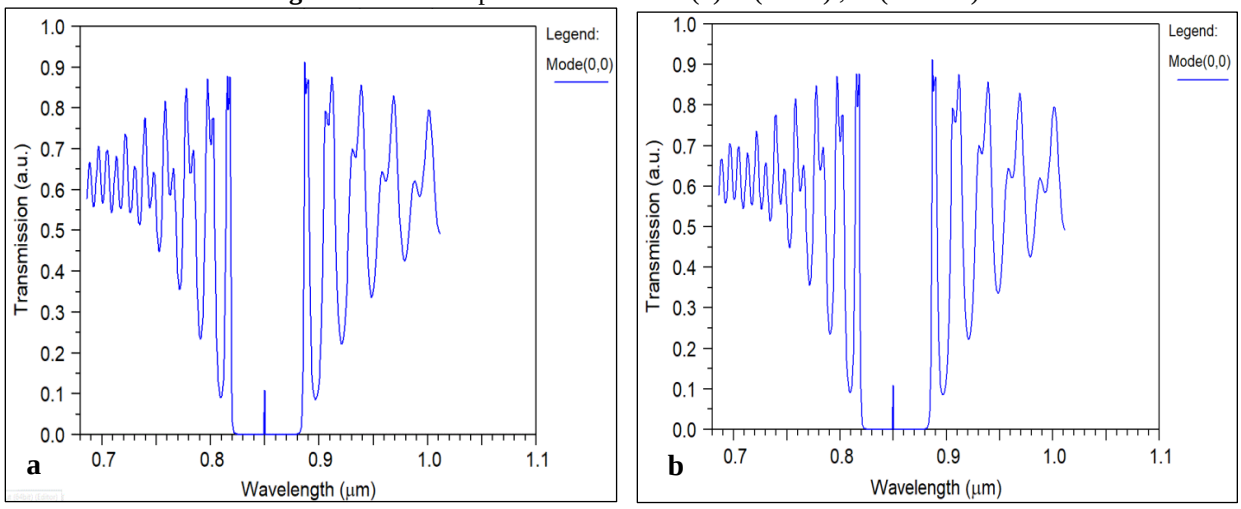

Figure 7. Transmission Spectra (At Bias0) a. (GaAs) ,b. (InGaAs).

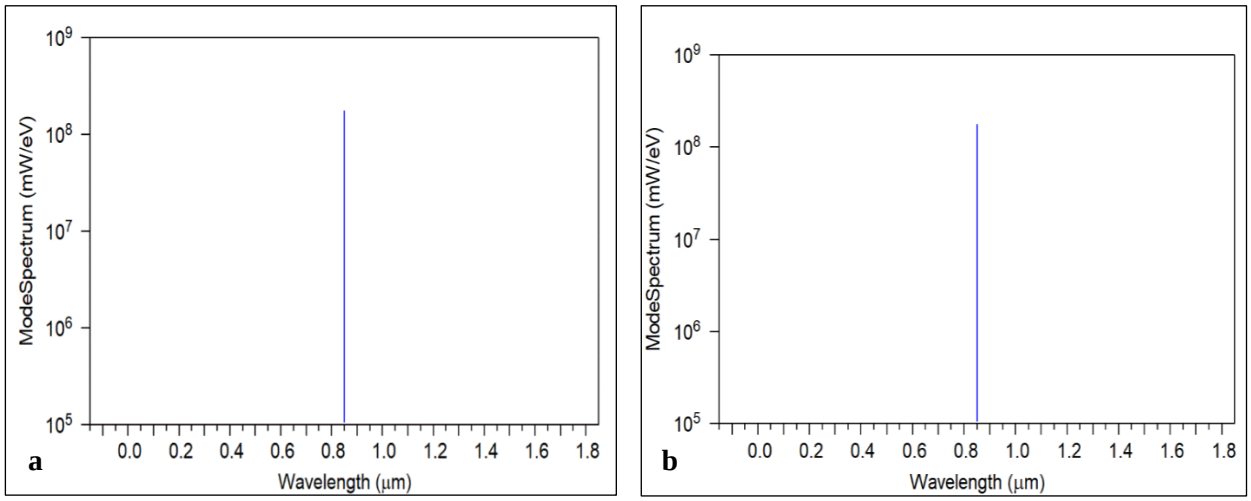

Figure 8. Optical Spectrum (at Bias 4) a. (GaAs) , b. (InGaAs).

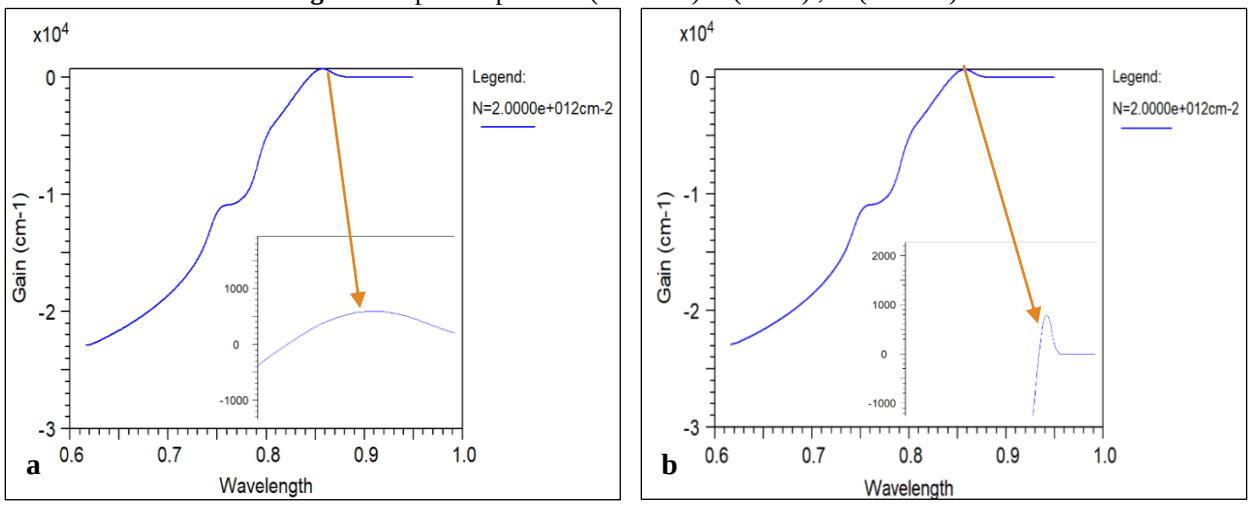

Figure 9. Material Gain a. (GaAs) , b. (InGaAs).

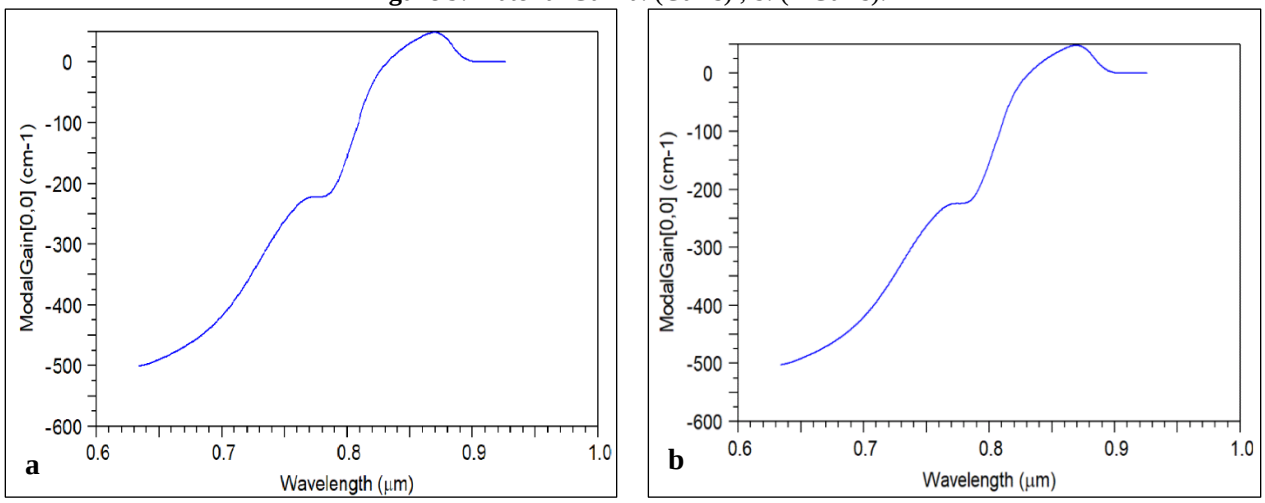

Figure 10. Modal Gain for Fundamental Mode (At Bias4) a. (GaAs) , b. (InGaAs).

4. Discussion

The results indicate that the VCSEL design, which uses InGaAs and GaAs as quantum well materials and an AlGaAs DBR, is effective in generating light emission at the desired wavelength of 0.85 µm. The optical mode stability and refractive index distribution indicate that the photonic cavity is an effective way to confine light in the active region, reducing internal losses and enhancing single-mode emission. The LIV curves at different temperatures show that GaAs performs well at low currents with stable emission at 300 K, while at 350 K the output

power reaches its maximum at 9.87 mA and then begins to decline at 10 mA. This behavior is consistent with what has been reported in previous studies[32]. In contrast, InGaAs exhibits superior performance at 350 K, reaching its maximum power at 10.1 mA and then declining at 10.2 mA, demonstrating its higher thermal stability and tolerance to high currents before the onset of heating effects. The decrease in output power at high injection currents in both materials reflects the well-known thermal rollover phenomenon caused by self-heating, which has been explained in specialized studies[33].The presence of a sharp peak in the photoemission spectrum at 0.850 µm confirms the efficiency of the cavity design, providing high spectral selectivity. The results also show that InGaAs has a higher gain compared to GaAs, reflecting its superior light amplification efficiency within the active region, while GaAs exhibits a lower gain due to its larger energy gap. Furthermore, the local gain of the fundamental mode was found to be enhanced at a wavelength close to 0.87 µm, which explains the interaction between the material properties and the cavity resonance, and represents a natural variation between the material's maximum gain and the cavity wavelength. In summary, these results indicate that the selection of quantum well materials and a well-calculated, optimized DBR structure are key factors in improving light emission efficiency and pattern stability. Moreover, the design can operate optimally under current and temperature influences, making it suitable for short-range, high-speed optical communication applications.

5. Conclusion

This work demonstrates that Laser MOD software is a powerful simulation tool to model and optimize VCSELs which provides accurate pre-fabrication performance predictions. For simplicity, only two materials can serve as QW InGaAs (Eg=1.409ev) And GaAs (Eg=1.424ev) for operating wavelength of 0.850µm. AlGaAs can be tuned for DBR having a thickness layer of λ/4 And period of λ/2. The study was particularly directed towards the examination of the effects of the critical structural parameters like cavity length (Lc), oxide aperture diameter (Dead), doping concentration (Nd) on the optical performance of the device. It was found that the optimized 1D VCSEL structures could obtain low-threshold current, single transverse mode, and high-quality Gaussian-like far-field emission, which is suitable for short reach optical communication. The size of the cavity was optimized to be about 8.6 µm in length and the of radius oxide aperture was approximately 10 µm demonstrate a good compromise between modal confinement, threshold current, and beam quality. The far-field profile and mode properties verified the possibility of this design to achieve an efficient coupling to multimode optical fibers, which is indispensable for DC and LAN. Further work can involve thermal effect analysis, dynamic modulation study, and the extension of the design for longer wavelengths, i.e., 0.980µm and 0.131µm, for more wide application in the optical interconnects and sensing applications.

Conflict of Interest

The authors declare that they have no conflicts of interest.

Funding

No funding.

Ethical Clearance

The authors declare nor conflicts of interest. The authors do confirm that I (or my) have read the corresponding author. (for all authors): I take public responsibility for the content of the manuscript, especially this: enough to believe the following the figures and tables are whose mine their statements are true about the study, especially: I confirm that the responsibility of the originality of my manuscript or the article references, especially, I attest to that we so attest that

each figure and table in the manuscript is our or my and that it is has no conflict figures and table in tersest.

References

1. Gullino A. Modeling and design of next-generation VCSELs: novel approaches for improved efficiency and reliability [PhD thesis]. Torino (IT): Politecnico di Torino; 2023. https://webthesis.biblio.polito.it/26772/
2. Li J, Zhao J, Gao F. Numerical investigation of optical and photoelectric properties for 850 nm VCSELs with arbitrary crystal orientation. Crystals. 2022;12(10):1459. https://doi.org/10.3390/cryst12101459
3. Chen Y, Pan Y, Wang F. Thermo-optical modeling of high-power VCSELs using coupled FEM simulation. Opt Express. 2021;29(4):5678–5690. https://doi.org/10.1364/OE.415678
4. Dohle R, Henning G, Wallrodt M, Gréus C, Neumeyr C. Advanced packaging technology for novel 1-dimensional and 2-dimensional VCSEL arrays. IMAPS Int Symp Microelectron. 2021;2021(1):000265. https://doi.org/10.4071/imaps.2021.000265
5. Du S, Su J, Zhou H, Zhang H, Qiu P, Deng J, Kan Q, Xie Y. Temperature-dependent characteristics of the high-speed 850 nm VCSEL. Proc SPIE. 2024;13183:1318309. https://doi.org/10.1117/12.303397
6. Hasan MM. Beam steering using dielectric and hybrid dielectric-metal Huygens' metasurfaces [Master's thesis]. Berkeley (CA): University of California, Berkeley; 2022. https://www2.eecs.berkeley.edu/Pubs/TechRpts/2022/EECS-2022-111.html
7. Xue I, Zhou Y, Zhang X, Zhang J, Zeng Y, Ning Y, Wang L. High-power single-mode 894 nm VCSELs operating at high temperature (>2 mW @ 365 K). Appl Phys B. 2022;128:16. https://doi.org/10.1007/s00340-021-07748-w
8. Szczygieł R, Sarzała R. Comprehensive electro-thermal-optical modeling of 850-nm VCSELs using self-consistent FEM. Opt Quantum Electron. 2020;52:211. https://doi.org/10.1007/s11082-020-2281-2
9. Jin D, Hong F, Zhang W, Zhang H, Wang Y, Wang H, Wang K, Guan B. Advances in thermal design of vertical cavity surface emitting laser array. Laser Technol. 2024;48(6):777–789. https://doi.org/10.7510/jgjs.issn.1001-3806.2024.06.002
10. Paul S, Haidar MT, Cesar J, Malekizandi M, Koegel B, Neumeyr C, Ortsiefer M, Küppers F. Far-field, linewidth and thermal characteristics of a high-speed 1550-nm MEMS tunable VCSEL. Opt Express. 2016;24(12):13142–13156. https://doi.org/10.1364/OE.24.013142
11. Wang X, Yang Q, Zhang W. 18 dB CW Raman on-off gain in silicon-on-insulator nanowire waveguide laser amplifiers. Opt Express. 2016;24(23):A1467–A1473. https://doi.org/10.1364/OE.24.0A1467
12. Mohammed AN, Anter FH. Simple mathematical technique in laser cavity design and manufacturing. Baghdad Sci J. 2006;3(3):23. https://doi.org/10.21123/bsj.2006.735
13. Hasan MA, Abood HA, Abdella GS, Shail MM. Theoretical study of the heating effect of laser radiations on SiUcaGlass systems. Baghdad Sci J. 2004;1(1):14.
14. Mahdi SS, Hamad IA. A laser induced fluorescence design for renewable energy application. Karbala Int J Mod Sci. 2020;6(3):Article 9. https://doi.org/10.33640/2405-609X.1707
15. Xu J, McCulloch D, Charlton MDB. Modeling full PCSELs and VCSELs using modified rigorous coupled wave analysis. Opt Express. 2024;32(13):22169–22180. https://doi.org/10.1364/OE.522484
16. Mu J, Zhou Y, Chen C, Zhang X, Zhang J, Liu T, Zhang Z, Xu Y, Yuan G, Zhang J, Ning Y, Wang L. Simulation of modal control of metal mode-filtered vertical-cavity surface-emitting laser. Sensors. 2024;24(14):4700. https://doi.org/10.3390/s24144700
17. Pomplun J, Burger S, Schmidt F, Schliwa A, Bimberg D, Pietrzak A, Wenzel H, Erbert G. Finite element simulation of the optical modes of semiconductor lasers. Phys Status Solidi B. 2010;247(4):846–853. https://doi.org/10.1002/pssb.200945451
18. Areebi NA, Jabir JN. Bandwidth improvement of a cone-inverted cylindrical and cross hybrids dielectric resonator antennas. Iraqi J Phys. 2023;21(1):77–87. https://doi.org/10.30723/ijp.v21i1.1084
19. RSoft Design Group. LaserMOD 9 user guide. RSoft Design Group, Inc.; 2012. https://www.synopsys.com/photonic-solutions/rsoft-photonic-device-tools/active-device-lasermod.html

20. Zhang Y, Li H, Wang J, Chen X. Thermal analysis and optimization of vertical-cavity surface-emitting lasers with different packaging structures. Chin J Lumin. 2024;45(8):1371–1379. https://doi.org/10.37188/CJL.20240141
21. Kandiah K, Menon PS, Shaari S, Yeop Majlis B. Design and modeling of a vertical-cavity surface-emitting laser (VCSEL). In: Proc ICSE; 2008. p. 297–302. https://doi.org/10.1109/ICSE.2008.4611053
22. Chung T, Won Y, Kim S. Single-mode VCSEL design optimization for short-reach data transmission. IEEE Photonics J. 2018;10(3):1–9. https://doi.org/10.1109/JPHOT.2018.2834215
23. Ledentsov NN, Makarov O, Shchukin VA, Kalosha VP, Ledentsov N Jr, Chorchos Ł, Bou Sanayeh M, Turkiewicz JP. High speed VCSEL technology and applications. J Lightwave Technol. 2022;40(6):1749–1763. https://doi.org/10.1109/JLT.2022.3149372
24. Kwon O, Moon S, Yun Y, Nam Y, Kim N, Kim D, Choi W, Lee J. Highly efficient thin-film 930 nm VCSEL on PDMS for biomedical applications. Sci Rep. 2023;13(1):571. https://doi.org/10.1038/s41598-023-27589-1
25. Wen C, Li W, Dai J, Ma S, Wang Z. Study on supermode control of external cavity VCSEL array with parallel-coupled model. Photonics. 2023;10(2):115. https://doi.org/10.3390/photonics10020115
26. Lu H, Alkhazragi O, Lin H, Ng TK, Ooi BS. Shaping the light of VCSELs through cavity geometry design. Light Sci Appl. 2025. https://doi.org/10.1038/s41377-025-01996-7
27. Pang C, Yan C, Yang J. New electrode structure vertical cavity surface emitting semiconductor laser and its array. J Phys Conf Ser. 2024;2921:012014. https://doi.org/10.1088/1742-6596/2921/1/012014
28. Grabherr M, Jager R, Peter M. High-power VCSEL arrays: thermal behavior and design optimization. IEEE Photonics Technol Lett. 2019;31(10):779–782. https://doi.org/10.1109/LPT.2019.2908475
29. Dąbrówka D, Sarzała RP. Study on bottom distributed Bragg reflector radius and electric aperture radius on performance characteristics of GaN-based vertical-cavity surface-emitting laser. Materials. 2024;17(13):3107. https://doi.org/10.3390/ma17133107
30. De Leonardis F, Passaro VMN, Magno F. Improved simulation of VCSEL distributed Bragg reflectors. J Comput Electron. 2007;6(3):289–292. https://doi.org/10.1007/s10825-006-0121-7
31. Lang R, Kobayashi K. External optical feedback effects on semiconductor injection laser properties. IEEE J Quantum Electron. 1980;16(3):347–355. https://doi.org/10.1109/JQE.1980.1070137
32. Abusaa M. Dynamical and thermal properties of 850 nm vertical cavity surface emitting laser (VCSEL). J Arab Am Univ. 2017;3:1–9.
33. Baveja PP, Kögel B, Westbergh P, Gustavsson JS, Haglund Å, Maywar DN, Agrawal GP, Larsson A. Assessment of VCSEL thermal rollover mechanisms from measurements and empirical modeling. Opt Express. 2011;19:15490–15505. https://doi.org/10.1364/OE.19.015490